VISUALIZATION OF SOIL EROSION UNDER A GEOTEXTILE DUE TO INFILTRATION USING X-RAY CT

Toshifumi Mukunoki[1], Noriaki Taniguchi[2], Hidetoshi Matsumoto[3] & Yutaka Murakami[4]

[1] *Kumamoto University. (e-mail: mukunoki@kumamoto-u.ac.jp)*
[2] *Kumamoto University. (e-mail: 072d8830@eng1.stud.kumamoto-u.ac.jp)*
[3] *Kumamoto University. (e-mail: matsu@tech.eng.kumamoto-u.ac.jp)*
[4] *Tanaka Co. Ltd. (e-mail: y.murakami@geo-tanaka.co.jp)*

Abstract: Stabilization of burned ashes in a landfill is related to the long-term infiltration through the cover-soil system. The long-term infiltration would cause three potential issues: dilution of pollution concentration in the leachate, erosion of fine grains in the final cover-treatment soil and melting/bonding of ash particles. The first factor is called "washing out effect" and this effect would bring the contribution of early stabilization of a burned ash. Meanwhile, the second and third factors would cause negative issue; namely, water path is locally developed in a waste and the final cover-treatment soil. Local generation of water path makes stabilization of the burned ash incline; therefore, the stabilization process promotes heterogeously. Hence, it is significant to reduce the generation of water path in the final cover-treatment soil. Recently, geotextiles have been used to reduce the erosion of soils and to disperse infiltration homogeneously in the ground. However, there is a paucity of research with respect to the generation of water path in landfill. To evaluate water-dispersivity effect of geotextile it is important to observe the erosion status in the final cover-treatment soil and to understand the generation mechanism of water path.

The objective of this study is to understand the factors to cause the early stabilization of the burned ash in the landfill due to long-term infiltration. As the first step, model infiltration tests using sands as a final cover-treatment soil was performed and the inner condition of model ground was scanned by X-ray Computed Tomography (CT) scanner, which can evaluate the density distribution of soils without any destruction. This paper will show cross-sectional images of model ground tested and the results of image analysis will give readers the density change of model ground with / without a geotextile due to infiltration.

Keywords: erosion control, geotextile, cover, landfill, non-destructive test

INTRODUCTION

Harmlessness of burned ashes in a landfill is related to the long-term infiltration called washing effect through the cover-soil system (Hanashima and Furuichi, 2004 and Higushi, 2005). The long-term infiltration such as rainfall would cause three potential issues: dilution of pollution concentration in the leachate, erosion of fine grains in the final cover-treatment soil and melting/bonding of ash particles. Washing effect would bring the contribution of early stabilization of a burned ash (McDougall et al. 2001). Meanwhile, the second and third factors would cause negative issue; namely, water path is locally developed in the final cover-treatment soil and eventually in a waste (Koener and Daniel, 1997). Local generation of water path makes harmlessness part of the burned ash incline; therefore, the harmlessness process of waste promotes heterogeously. Hence, it is significant to reduce the generation of water path in the final cover-treatment soil. Recently, geotextiles have been used to reduce the erosion of soils and to disperse infiltration homogeneously in the ground (Kavazanjian et al. 2006 and Heibram et al 2006). However, there is a paucity of research with respect to the generation of water path in landfill.

This paper will discuss the result of model infiltration tests using sands as a final cover-treatment soil using X-ray Computed Tomography (CT) data. Cross-sectional CT images of model ground tested and the results of image analysis will give readers the density change of model ground with / without a geotextile due to infiltration.

TESTING METHODS

Test materials

In this study, two different conditions of model ground were prepared such as non-placing a geotextile (herein refer as case 1) and placing the geotextile (herein refer as case 2) on the model ground to evaluate the reduction effect of water path in the model ground. The geotextile tested was non-woven type made of polyether and its thickness was 10 mm. The porosity was 0.9 and the characteristic opening size was 0.2 mm.

Soil material was called Soma sand and the particles with mean diameter (D_{50}) of 106μm as fine grains and 2mm and coarse grains were regulated in 1 : 5. The regulated dry sands were pored into the soil box by a shovel to avoid inclining the large particles in the model ground. The dimension of the model ground was 120mm in height and 130mm in diameter and the bulk dry density was 1.67 t/m^3.

Test apparatus and procedure

Figure 1 illustrates the schematic of the test apparatus. In order to evaluate the water dispersivity of geotextile, the nozzle with 0.6 mm diameter of single hole was used for infiltration test. After instillation of sand into the soil box, the model ground was carried to the CT room and scanned as the initial condition. Scanning locations were from the boundary between drainage layer and model ground for the model to 20mm, 40mm and 70mm. As for scanning a geotextile, it was scanned every 1.0 mm from the surface to the bottom of geotextile and totally ten image were

obtained (i.e. the thickness of geotextile was 10 mm). To understand the progress of soil erosion, the model ground was scanned at 0 min. as initial condition, 1 min., 6 min., 13min., and 20 min. The fine grains were observed in the outflow water at the bottom of soil box until 13 min. after and the test was terminated at 20 min. because no fine grains were observed.

In the case 2, a geotextile was placed on the surface of the model ground and there was no restriction to horizontal direction for water migration due to local infiltration in this test.

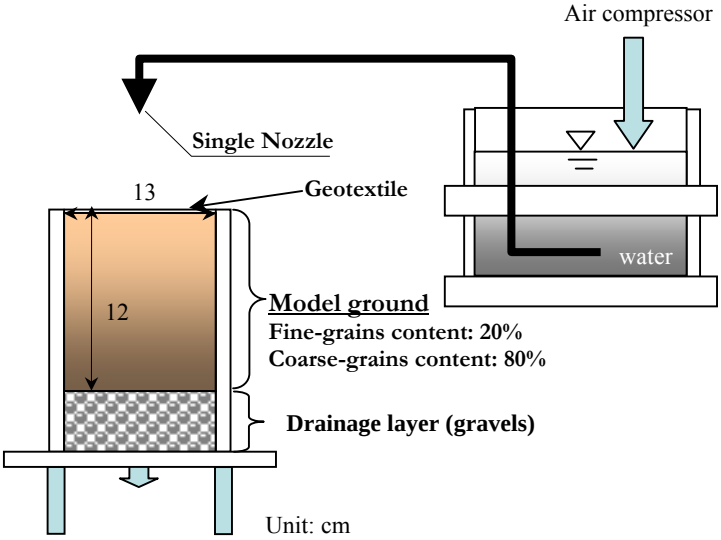

Figure 1. Schematic of a test apparatus

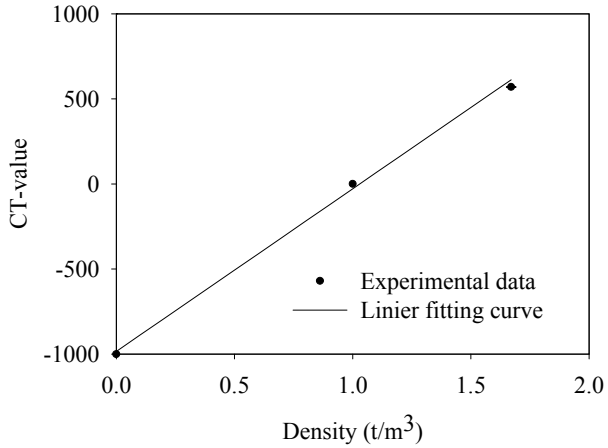

Figure 2. Correlation between CT-value and sample

Table 1. The specification of X-ray CT scanner

Scan type	Traverse/Rotation
PowerVoltage for generation of x-ray beam	300 /200 /150 kV
Number of detectors	176 channels
Maximum size of the specimen	D:400mm (ϕ = 150 or 400)×H:600mm
Number of voxel	512x512, 1024x1024, 2048x2048
Pixel size for ϕ = 150 mm	70μm, 140μm, 293 μm
Thickness of X-ray beam (mm)	0.3 ,0.5, 1.0, 2.0, 4.0 mm
Scan time (half, full, double)	2.5, 5.0, 10.0 min.
Spatial resolution	0.2mm (diameter of the hole) for 20mm thickness of steel

Summary of x-ray CT scanner

CT-value and X-ray CT image (Otani. et al, 2000 and Mukunoki et al, 2003)

The output of X-ray CT analysis is an x-ray attenuation coefficient (μ) at each different special location in the specimen and it is well-known that the x-ray attenuation coefficient (μ) is a linier relation to the density of the material. Lenoir et al. (2007) described the issue of x-ray attenuation coefficient in detail. In the CT system installed at Kumamoto University, the CT-value is defined by the following equation:

$$CT-value=(\mu_t-\mu_w)K/\mu_w \quad (1)$$

where μ_t : coefficient of absorption at scanning point; μ_w : coefficient of absorption for water; and K ; material constant. It is noted that the coefficient of absorption for air is zero for the condition of K =1000 and then, the CT-value of the air is -1000. Figure 2 shows that the CT-value also has linear relationship to the density of bulk density regulated in this study. The CT-value for each location in the specimen is given to the voxel and the aggregation of voxel is the X-ray CT image. The CT-values can be shown on each voxel as black and white in 256 grey level colours. Noted that the display level can be changed by a CT users valuably; hence the CT users should check the range of CT-value obtained to show the image accurately and to do quantitative discussion.

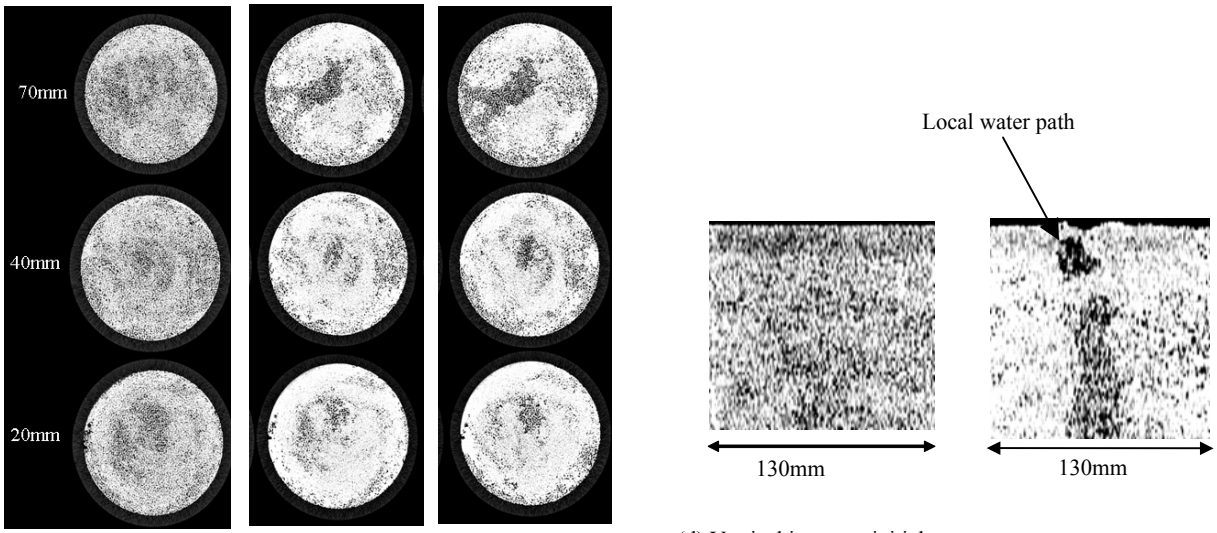

(a) Initial (b) 1 min. (c) 6min. (d) Vertical image at initial condition (e) Vertical image at 20 min. after

Figure 3. X-ray CT images of model ground due to local infiltration without

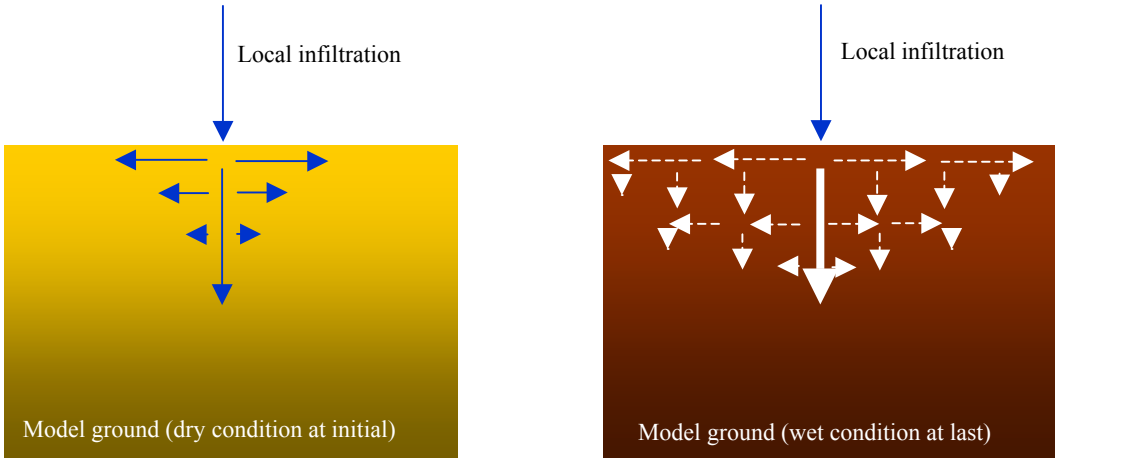

(a) Initial behaviour of water (b) Behaviour of water migration at the equilibrium condition

Figure 4. Illustration of water migration due to local

RESULTS AND DISCUSSION

Soil erosion due to local infiltration

Figure 3(a), (b) and (c) show the X-ray CT images of the model ground in each height as Case1 at the status of the initial condition, 1 minute after and 6 minutes after and Figure 3(d), (e) show the vertical image of model ground at initial condition and 20 minutes after, respectively. It can be observed that the brightness of images at 1 min. and 6 min. more than that at the initial condition. Water dropped to the model ground through a single nozzle. Once water reached the ground surface, water migrated to the depth direction and horizontal direction due to capillarity of sandy soil and the wet bulk density of model ground increases. Hence, the CT images at 1 min. and 6 min. after as shown in Figure 3 (b) and (c) look white. Likewise, the CT-value evaluates the density but cannot distinguish the dry density from wet density without using the calibration data such as shown in Figure 2.

Meanwhile, the black area can be observed in the center of the CT images in Figure 3 (b), (c) and (e). This visualizes the water path due to local infiltration. Despite that the water dropped at the single point on the ground surface, the shape of black area is not circle but complex as shown in Figure 3(b) and (c). Herein, there are two behavior of infiltration as shown in Figure 4. As the initial behavior of water migration, water dispersed due to capillarity to the horizontal direction and then its water started to went down to the bottom of the soil box. The water migration in the model ground just underneath of local infiltration dominantly creates the water path because of erosion of the fine grains and Figure 3 (e) proves it. It can be seen that the water path as shown in Figure 3(e) was visualized discontinuously. This could be caused because of inhomogeneous condition of model ground and the water path was not only straight progressing but also horizontal progressing as shown in Figure 3(b) and (c).

Figure 5 presents the histogram of CT image at initial condition and 20 min. after. The histogram can be categorized 3 ranges as shown in Figure 5. The CT-value of model ground after 20min. is shifted to right side and this means the bulk density of model ground increased from initial condition to the status at 20 min. after. However, region (a) as shown in Figure 5 has opposite tendency and this indicates that the low density area increased locally. Theoretically, the CT-values for water and air are 0 and -1000, respectively. Hence, region (a) in Figure 5 indicates that porosity filled with air or water increased in this test. However, the dimension of a voxel in this study was 0.293 x 0.293 x 1.0 mm^3 so the X-ray CT scanner used in this study does not have enough resolution to distinguish soil particle and porosity. At least, the region (a) in Figure 5 after 20min. means the low density area created newly due to local infiltration and it is 6.4 % to entire area in CT image of the model ground. As for the region (b) in Figure 5, there are two issues herein. The first issue is simply CT-value shifted to the right side and the second issue is the frequency of CT-value decreases. The reduction of the frequency of CT value does also means the decrease of bulk density. More discussion will be need to distinguish the first issue to second one, but at least the CT images as shown in Figure 3 presented the water path.

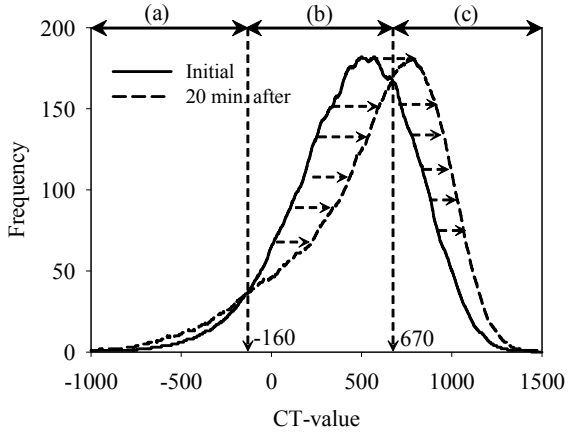

Figure 5. Change of CT-value histograms for

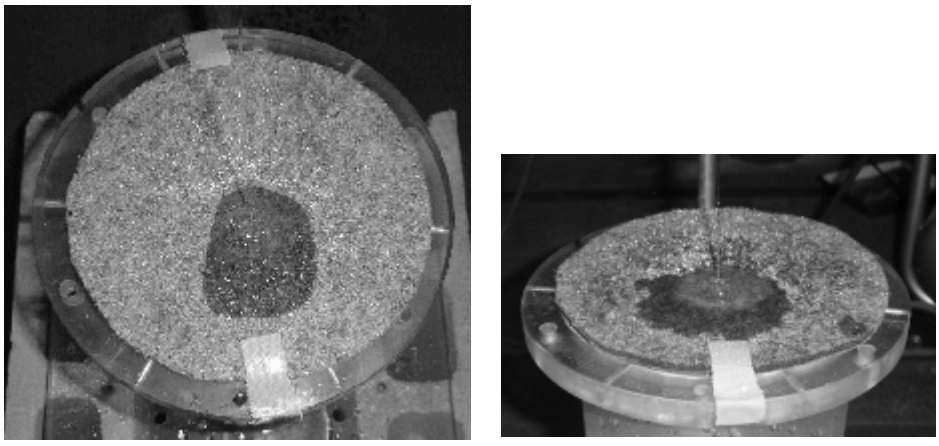

(a) Plane view from the top

(b) Side view from the top

Figure 6. Photographs of geotextile due to local

Soil erosion due to local infiltration underneath a geotextile

Figure 6 presents photographs of a geotextile tested with pouring from the single nozzle after 6 min.. It can be seen that water dispersed locally. In fact, the dark part in geotextile as shown in Figure 6 almost saturation condition and the part around the dark part was not dry condition but unsaturated condition. Probably, the water in the model

ground underneath the geotextile saturated migrate into the ground dominantly likewise Case 1. However, the surface tension of water would cause the reduction of water dropping into the ground from the geotextile.

Figure 8 shows the X-ray CT images of the model ground in each height as Case 2 at the status of the initial condition, 1 minute after and 6 minutes after and Figure 8(d), (e) show the vertical image of model ground at initial condition and 20 minutes after, respectively. The dark area such as shown in Figure 3 (b) and (c) cannot be observed in Figure 8 (b), (c) and (e), clearly. Meanwhile, Figure 7 presents the histogram of CT image at initial condition and 20 min. after for Case 2. The histogram can be categorized 3 ranges as well as Case 1; however, the region (a) in Figure 7 could not detect such as Figure 5. This concluded that the low density area did not create newly due to local infiltration because the effect of water dispersivity to the horizontal direction and t water drop reduced into the ground from the geotextile because of surface tension of water. In short, the geotextile played to change to multi-infiltration from the single local infiltration. However, the issue as for region (b) in Figure 7 discussed in the previous section as for Figure 5 remains still. Figure 9 presents the 3-dimension X-ray CT image of geotextile tested at each stage, Figure 8 (b), (d) and (f) present only water part in the geotextile. It is available to extract only water part from the geotextile because X-ray CT image is a digital image and then, the geotextile is highly porous material so the resolution issue was negligible. In fact, Figure 7(e) shows that grey area in the center of the vertical image and this location is almost correspond to the saturated area in geotextile as shown in Figure 6; therefore, there would be a tendency to create the water path due to dominant infiltration.

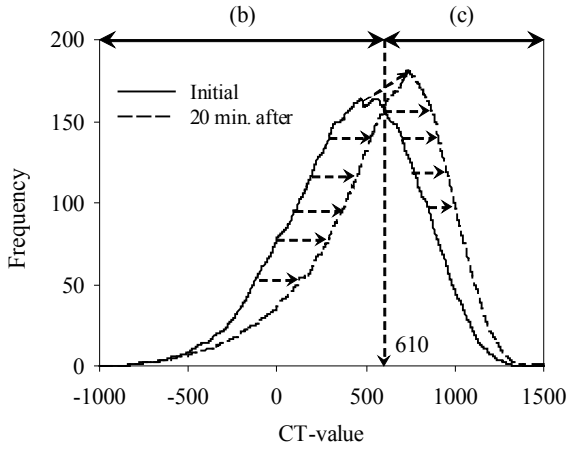

Figure 7. Change of CT-value histograms for

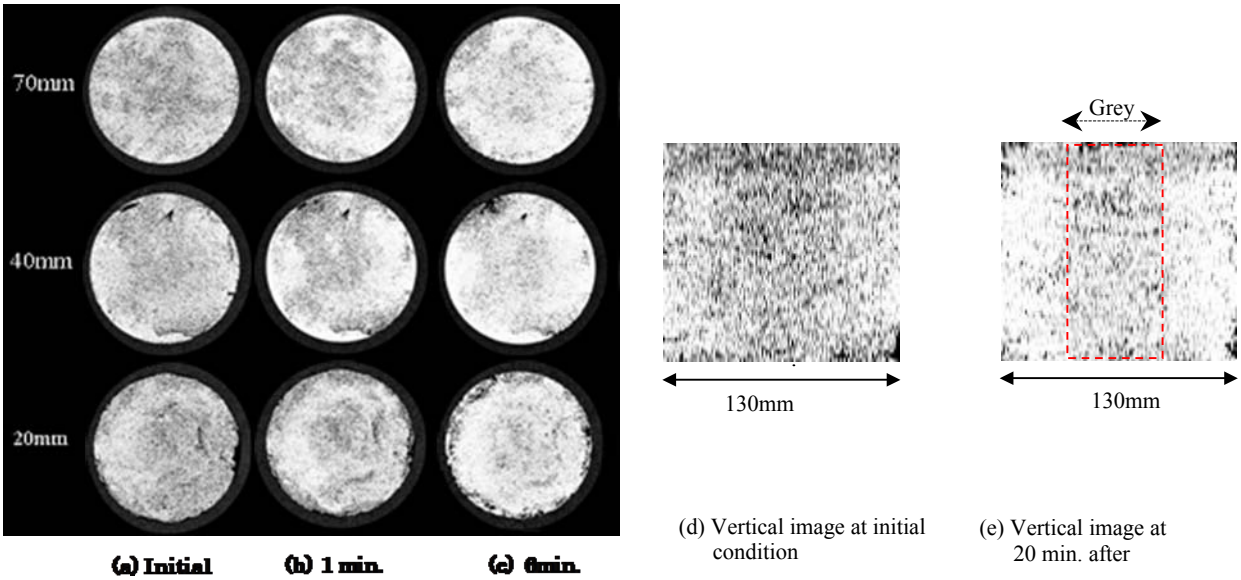

Figure 8. X-ray CT images of model ground underneath a geotextile due to local infiltration

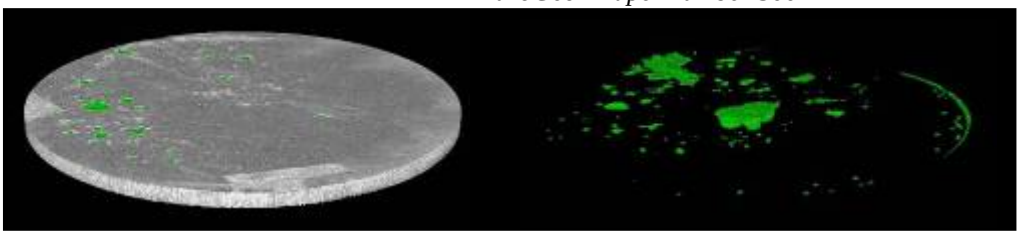

(a) Entire geotextile sample after 1 min.

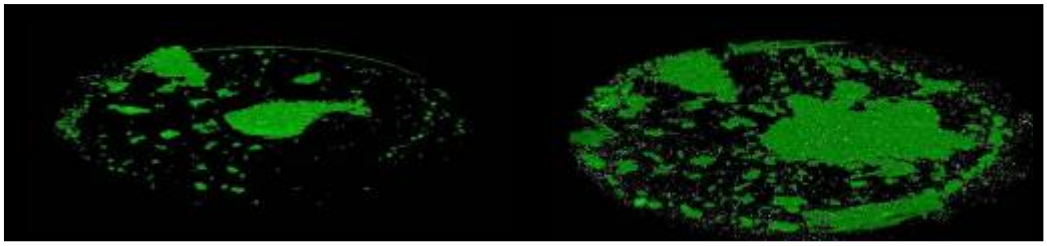

(c) Wet area in the geotextile sample after 6 min.

Figure 9. 3-D X-ray CT images of geotextile sample and wetting area

CONCLUSIONS

The soil erosion test with model sandy ground due to local infiltration using a single nozzle was performed and the inner condition of model grounds at each level was scanned by X-ray CT scanner. Water path could be visualized in the case of without using a geotextile. The conclusions in this paper are summarized as follows:

(1) X-ray CT scanner is effective application to visualize the soil erosion;
(2) The behavior of fine soil which go through between coarse soil is predominant due to local infiltration;
(3) It is necessary to distinguish CT-value with respect to change from high density to low density due to wetting in the model ground from CT-value to wet-bulk density; and,
(4) A geotextile has water dispersivity and reduction effect to local infiltration; however, there is a possibility that water path would be created in the case of long term infiltration.

Acknowledgements: Authors would like to thank Prof. J. Otani of Kumamoto University for his support and precious comments. Authors also would like to give their gratitude to Prof. Y. Obara of Kumamoto University and the head of GeoX CT Center for his support.

Corresponding author: Dr. Toshifumi Mukunoki, Kumamoto University, 1-39-2 Kurokami, Kumamoto, Kumamoto, 860-8555, Japan. Tel: +81-96-342-3545. Email: mukunoki@kumamoto-u.ac.jp.

REFERENCES

Hanashima, M. and Furuichi, T. 2004. Landfills in Japan, The landfill Systems & technologies research association of Japan, NPO.

Heibram, M., Fourie, A., Girard, H., Karunaratne, G.P., Lafleur, J. and Palmeira, E.M. 2006. Hydraulic applications of geosynthetics, Procs. of the 8th international conference on Geosynthetics (8ICG), Vol. 1, 79-120.

Higuchi, S. 2005. "Early stabilization for the landfill", Proc. of 17th Annual Conference of The Japan Society of Waste Management Experts, JSWME:959.(in Japanese)

Kavazanjian, Jr. E., Dixon, N., Katsumi, T. Kortegast, A., Legg, P. and Zanzinger, H. 2006, Geosynthetic barriers for environmental protection at landfills, Procs. of the 8th international conference on Geosynthetics (8ICG), Vol. 1, 121-152.

Koerner, R. and Daniel, D. 1997. Final covers for solid waste landfills and abandoned dumps", American Society of Civil Engineering.

McDougall, F., White, P., Frank, M. and Hindle P. 2001. Integrated solid waste management: life cycle inventory, Blackwell publishing Ltd, Oxford.

Mukunoki, T., Otani, J., Obara, Y. and Kaneko, K. 2003. X-ray CT data on assessment of geomaterials properties, Procs. of the International Workshop on X-ray CT for Geomaterials, GeoX2003, 85-90.

Otani, J., Mukunoki, T. and Obara, Y. 2000. Application of X-ray CT method for characterization of failure in soils, Soils & Foundations, Vol. 40, No.2, 113-120.